Electronic Supplementary Material (ESI) for ChemComm.

Supplementary Information

Rational design of a neutral pH functional and stable organic photocathode

Laia Francàs,‡[a]* Eric Burns,‡[a] Ludmilla Steier,[a] Hyojung Cha,[a] Lluis Solà-Hernández,[b] Xiaoe Li,[a] Pabitra Shakya Tuladhar,[a] Roger Bofill,[b] Jordi García-Antón,[b] Xavier Sala,[b] James R. Durrant [a]*

Correponding authors: lfrancas@ic.ac.uk; j.durrant@imperial.ac.uk

1. Experimental information:

A. Chemicals and reagents

$PC_{70}BM$ was purchased from Solenne BV, PCDTBT from 1-Material, PEDOT:PSS from Heraeus, evaporator materials from Kurt J. Lesker company, ultrasonic solder (alloy #GS155) from Cerasolzer, and 5-minute epoxy resin from Devcon. RuO_2 nanoparticles were synthesized by hydrothermal synthesis following a reported procedure.[1] All other materials and reagents were purchased from Sigma-Aldrich.

B. Device fabrication

Devices were prepared on cleaned ITO-glass substrates: ITO substrates were sonicated for 20 minutes in detergent water and followed by 3 sonicated washes of 5 minutes in DI water, 2 sonications of 5 minutes in acetone, and 1 sonication of 5 minutes in isopropanol. ITO-glass were then treated with an additional O_2 plasma treatment (8 min at 3 mbar O_2 at 155 W) immediately prior to device fabrication. OPV and OPV PEC devices were then constructed via subsequent spincoating/drying steps of different material layers. After each spincoated thin film, a narrow strip ~1 mm was removed using a complimentary solvent to reveal the ITO back contact as indicated in figure S1b. The final tested PEC devices were presenting an area between 0.6 to 0.7 cm^2.

NiO layer:

Nickel oxide (NiO) HTL solution was prepared from 52 mg nickel(II) acetate tetrahydrate in 1ml methoxyethanol and 12µl ethanolamine and stirred overnight. The NiO solution was filtered through a 0.45 micron PTFE filter and spincoated directly onto clean ITO at a spin speed of 4000 rpm for 45 s. A thin strip of the deposited film was wiped clean using isopropanol as indicated in figure S1b. NiO layers were annealed at 250 °C for 20 min and post-treated with O_2 plasma immediately prior to BHJ film deposition (8 min at 3 mbar O_2 at 155 W) which serves to shift the work function deeper – towards the HOMO energy level of the donor polymer.[1,2]

PEDOT:PSS layer

PEDOT:PSS was filtered through a 0.45 micron PTFE filter and otherwise used as received. The PEDOT solution was spincoated at a spin speed of 3500 rpm for 45 s onto ITO-glass. A thin strip of the deposited film was wiped clean using DI water (as indicated in figure S1b) and the remaining film was subsequently annealed at 150 °C for 15 min.

PCDTBT: $PC_{70}BM$ blend

A solution of PCDTBT: $PC_{70}BM$ (1:2) 18 wt% in chlorobenzene was prepared and stirred for at least 12h before use. Note: the same solution may be kept over a period of several days under a stirred environment with no apparent loss in performance. The blend solution was spun onto the hole selective layer at a spin speed of 2000 rpm for 60 s with no post-treatment.[3] A thin strip was wiped clean with chloroform to reveal the ITO back contact as indicated in figure S1b.

OPV fabrication:

Organic photovoltaic devices had the following structure: ITO || NiO or PEDOT:PSS || PCDTBT: $PC_{70}BM$ || Ca (25 nm) || Al (150 nm)

Calcium and aluminium contacts were thermally evaporated as shown in Fig. S1c.

Photocathode fabrication:

Organic photocathode devices had the following structure: ITO || NiO or PEDOT:PSS || PCDTBT: $PC_{70}BM$ || Au (70-80 nm) or ALD TiO_2 (100 nm) || RuO_2 NP

Gold was thermally evaporated onto the middle of the OPV cells to give a cumulative pixel area of 1 cm^2 (Fig. S2a).

Atomic layer deposition of TiO_2:

A layer of 100 nm TiO_2 was deposited via atomic layer deposition (ALD) in a home-built ALD reactor, at 75 °C hotplate temperature in exposure mode with pulse, hold and purge times of 0.015 s/10 s/60 s for H_2O (held at room temperature) and 0.1 s/10 s/60 s for tetrakis(dimethylamino) titanium, (TDMAT, heated at 75 °C) with 10 sccm N_2 flow.[4] A growth rate of 0.7 Å per cycle on a Si wafer as measured by a reflectometer (F20, Filmetrics). To avoid polymer degradation, the chamber was cooled to 30 °C before inserting and removing the samples. The substrates were heated only after evacuating the chamber to ~0.3 mbar under inert N_2 (Carbagas, 99.999% pure) flow. A thin strip of thermal tape was applied to the top of the photocathode device to prevent TiO_2 deposition onto the ITO back contact as seen in figure S2c.

RuO_2 deposition:

RuO_2 nanoparticles were prepared through a hydrothermal method previously published (Figure S3).[1] RuO_2 nanoparticles were added to 1 ml methanol at concentration 10 mg/ml and stirred for 48 h to create a suspension. 30 µl of the RuO_2 nanoparticles solution were spin-coated onto TiO_2- or Au-coated devices at 4000 rpm for 40 s. A thin wire soldered to the ITO back contact via ultrasonic soldering and the final device was encapsulated around the edges with epoxy such that only the solution-OPV interface layer was exposed to the electrolyte (Fig. S2b).The catalyst after deposition on top of our photocathode was activated by performing several LSV under 1 sun illumination (Figure S11).

C. Instrumentation:

XRD patterns of the samples were recorded at the "Servei de Difracció de Rais X" at the UAB using a Phillips XPert diffractometer equipped with a two circle diffractometers and a Cu tube.

Transmission electron microscopy observations were performed at the "Servei de Microscòpia" of the UAB. TEM grids were prepared by drop-casting of the crude colloidal solution onto a holey carbon-coated copper grid. TEM analyses were performed on a JEOL 2011 electron microscope working at 200 kV with a point resolution of 1.8 Å. Statistical size distributions were built via manual analysis of enlarged micrographs by measuring ca. 200 non-touching nanoparticles. The analyses were done by assuming that the nanoparticles are spherical. Nanoparticle sizes are quoted as the mean diameter ± the standard deviation.

Solar cell performance was evaluated under xenon lamp with AM 1.5G filters at 1 sun referenced to a certified silicon diode.

All photocathode electrochemical measurements were carried out in a cappuccino cell in a three-electrode configuration using an Ag/AgCl (sat'd KCl) as a reference, a Pt mesh as a counter and the photocathode as the working electrode in 0.1 M phosphate buffer (pH 7) or 0.1 M sulfuric acid (pH 1). Linear sweep voltammetry and chronoamperometry measurements were carried out with an Autolab PGSTAT101 potentiostat under simulated AM 1.5G illumination (1 sun calibrated with a certified Si diode using a KG3 filter).

Hydrogen evolution measurements were performed in a gas tight three electrode electrochemical cell with the best performing photocathode applying 0 V *vs* RHE under 1 sun back illumination. The hydrogen was detected using a gas-phase Clark-type hydrogen electrode (Unisense H_2-NP microsensor). Quantification of the evolved gas was done by adding known volumes of hydrogen.

D. Faradaic efficiency calculations

The Faradaic efficiency has been estimated as follows:

$$\mathrm{FE} = \frac{\text{moles of gas phase } \mathrm{H_2} + \text{moles of dissolved } \mathrm{H_2}}{\text{moles of } \mathrm{H_2} \text{ calculated from the photocurrent}} \text{ x } 100$$

Moles in the gas phase were directly estimated from the H_2 clark measurement =7.76 10^{-6} H_2 moles

Moles of dissolved H_2:

$$[\mathrm{H_2}] = \frac{\mathrm{P}}{\mathrm{K_H}}$$

Where K_H (Henry constant) = 1282.05 $\frac{\mathrm{L\ x\ atm}}{\mathrm{mol}}$, and P is the pressure in the head space of the cell

P was estimated using the ideal gases law:

$$\mathrm{P} = \frac{\text{moles } \mathrm{H_2} \text{ x R x T}}{\text{Volume}} = \frac{7.76 \text{ x } 10^{-6}(\text{moles}) \text{x } 0.082 \left(\frac{\mathrm{L\ x\ atm}}{\mathrm{K\ x\ mol}}\right) \text{x } 298 \text{ (K)}}{5.2 \text{ x } 10^{-3}(\mathrm{L})} = 0.0365 \text{ atm}$$

$$[\mathrm{H_2}] = \frac{\mathrm{P}}{\mathrm{K_H}} = \frac{0.0365 \text{ (atm)}}{1282.05 \left(\frac{\mathrm{L\ x\ atm}}{\mathrm{mole}}\right)} = 2.85 \text{ x } 10^{-5} \frac{\mathrm{mole}}{\mathrm{L}}$$

This concentration was in a 55 mL of aqueous solution, so 1.566 x 10^{-6} moles of H_2 were dissolved in the solution

From the monitored photocurrent we know that we have accumulated 15.55 coulombs which corresponds to 8.06 x 10^{-5} moles of H_2

$$\mathrm{FE} = \frac{7.76\ x\ 10^{-5} + 1.566 \text{ x } 10^{-6} \text{ moles of } \mathrm{H_2}}{8.06 \text{ x } 10^{-5}} \text{ x } 100 = 98\ \%$$

2. Tables and Figures

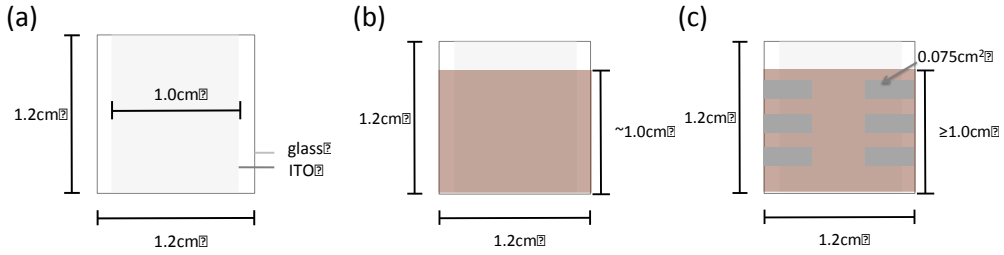

Figure S1. (a) Typical ITO glass slide used in this work. (b) Device with absorber blend. In case of the organic photocathode, the ALD TiO_2 layer would cover the same absorber area. (c) OPV device after calcium and aluminum thermal evaporation.

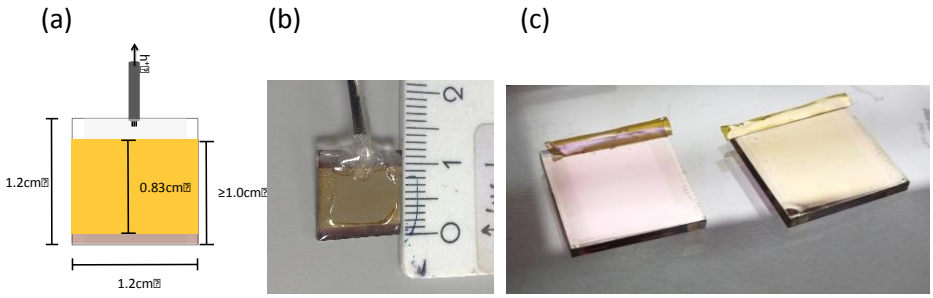

Figure S2. (a) Photocathode after thermal evaporation of gold. (b) Photograph of a photocathode device coated with Au and RuO_2 nanoparticles. (c) Photograph of photocathode device coated without (left) and with (right) TiO_2-ALD.

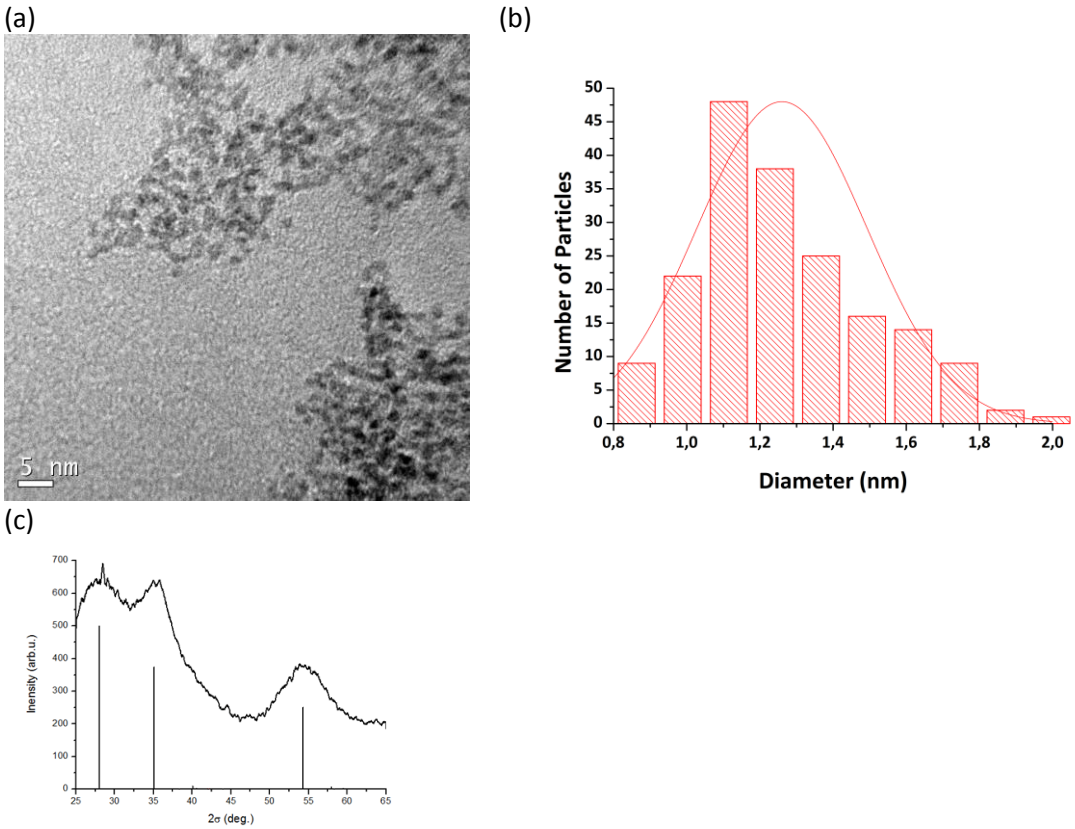

Figure S3. RuO_2-NP characterisation. (a) TEM image (b) size distribution histogram and (c) powder XRD diffractogram with RuO_2 theoretical pattern. The presented experiments show the rutile RuO_2 nature of the as synthesised 1.3 ± 0.3 nm nanoparticles.

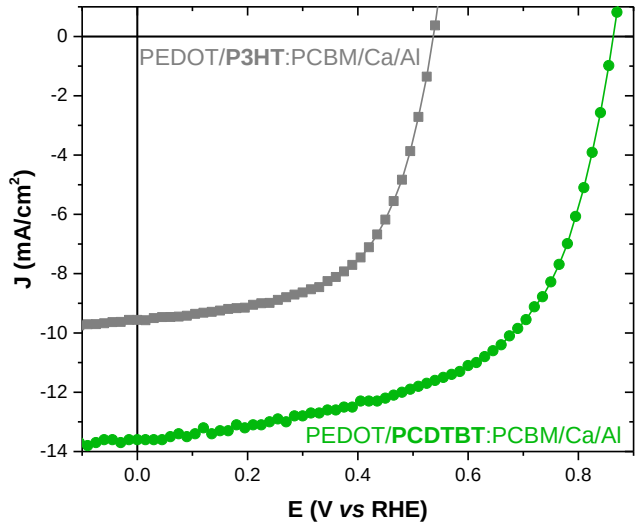

Figure S4. J-V curves for the conventional solar cell devices using P3HT:PCBM (grey) or PCDTBT (green).

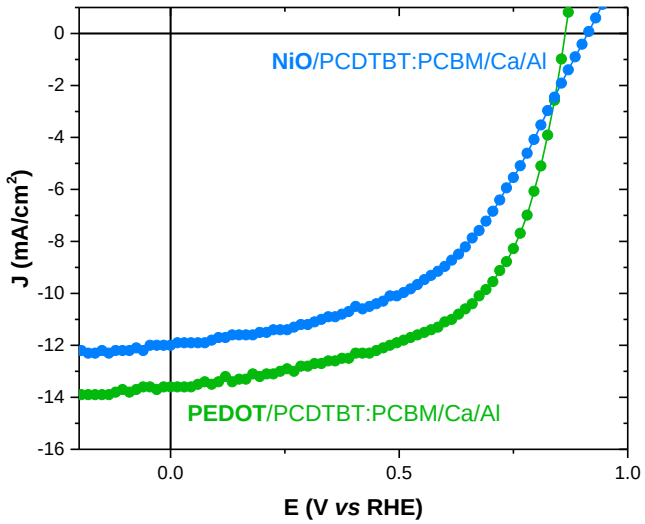

Figure S5. J-V curves for the conventional solar cell devices using PEDOT/PCDTBT:PCBM (green) or NiO/PCDTBT:PCBM (blue).

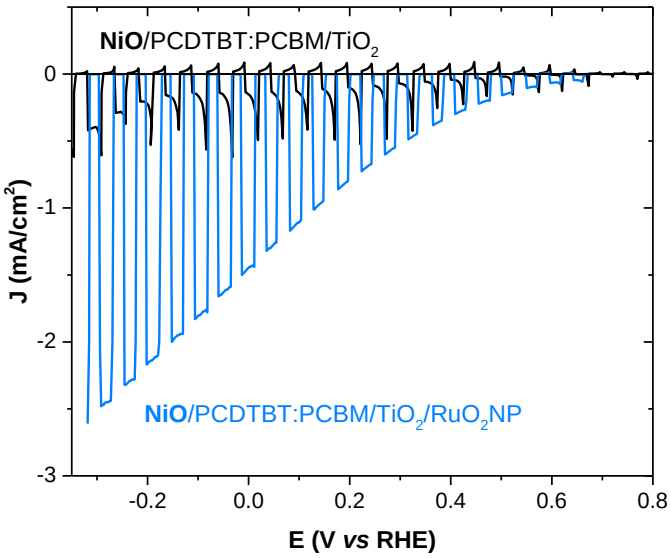

Figure S6. J-V curves at pH 7 using photocathodes with the conformation NiO/PCDTBT:PCBM/TiO_2 (black trace) and NiO/PCDTBT:PCBM/TiO_2/RuO_2-NP (blue trace) using back illumination (Area = 0.7 cm^2).

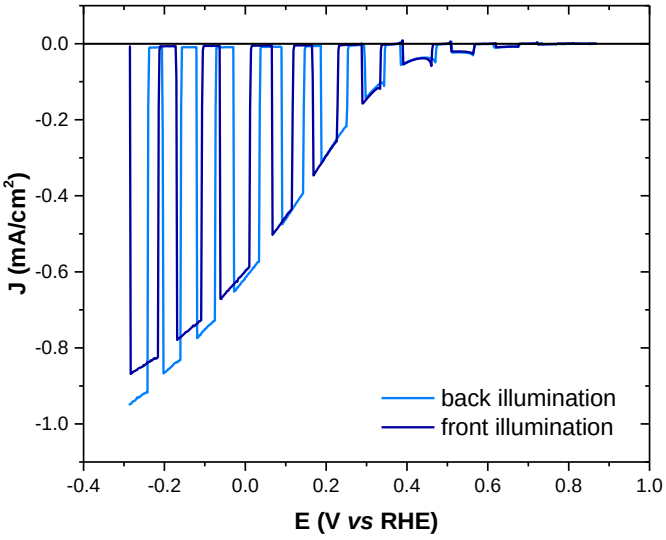

Figure S7. J-V curves at pH 7 using photocathodes with the conformation NiO/PCDTBT:PCBM/TiO_2/RuO_2-NP using front and back illumination (Area = 0.6 cm^2).

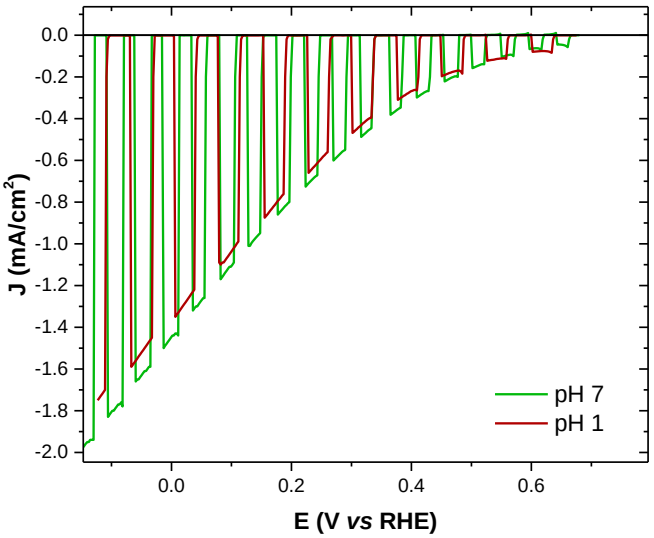

Figure S8. J-V curves using NiO/PCDTBT:PCBM/TiO_2/RuO_2-NP as a photocathode at pH 1 (red) and pH 7 (green), back illumination (Area = 0.7 cm^2).

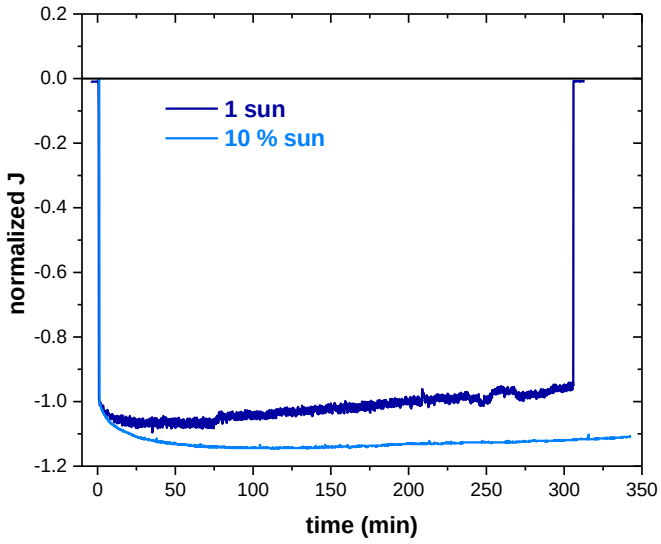

Figure S9. Bulk electrolysis at 0 V vs RHE at 1 sun (dark blue) and 10% of a sun (light blue) (Area = 0.7 cm^2).

(a)

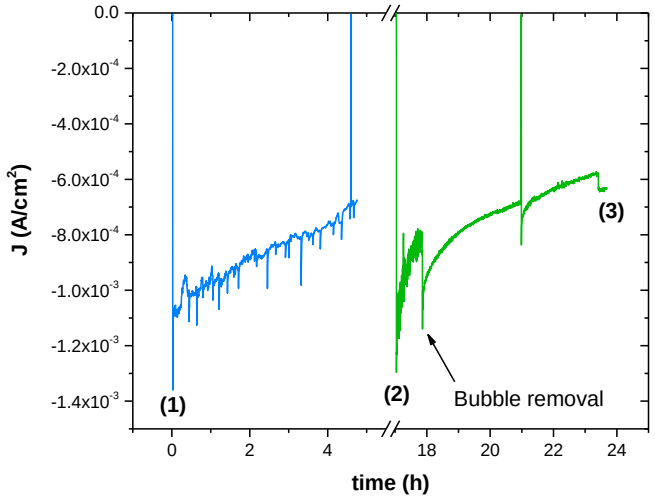

(b)

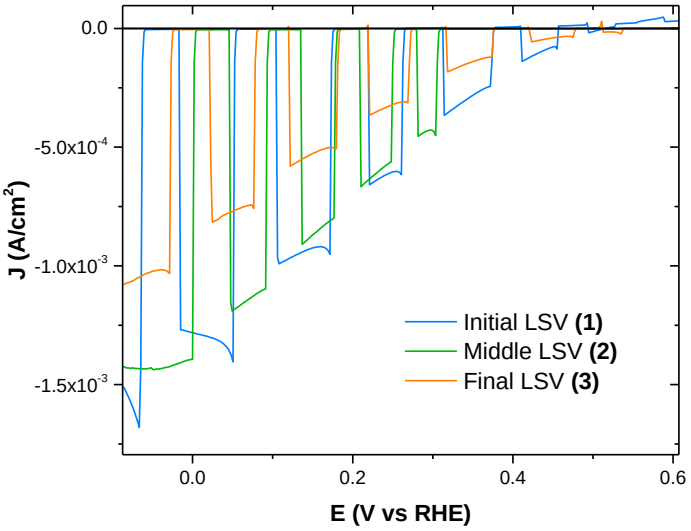

Figure S10. Long term bulk electrolysis experiment performed with a NiO/PCDTBT:PCBM/TiO_2/RuO_2-NP **[2]** at 0 V vs RHE at 1 sun. (a) Current density *vs* time during two consecutive 5 h bulk electrolysis, 1-5 hours (light blue) and 5-10 hours (green). (b) LSV before the experiment (light blue), after 5 h of bulk electrolysis (green) and after 10 h of bulk electrolysis (orange). The initial 5 hours decay can be associated with bubble formation, as indicated by the lack of deactivation measured by the LSV before (light blue) and after (green) this first 5 hours of bulk electrolysis. In the next 5 hours of electrolysis (green) the decay of performance is due to some deactivation of the system and is around 20%. (area 0.7 cm^2).

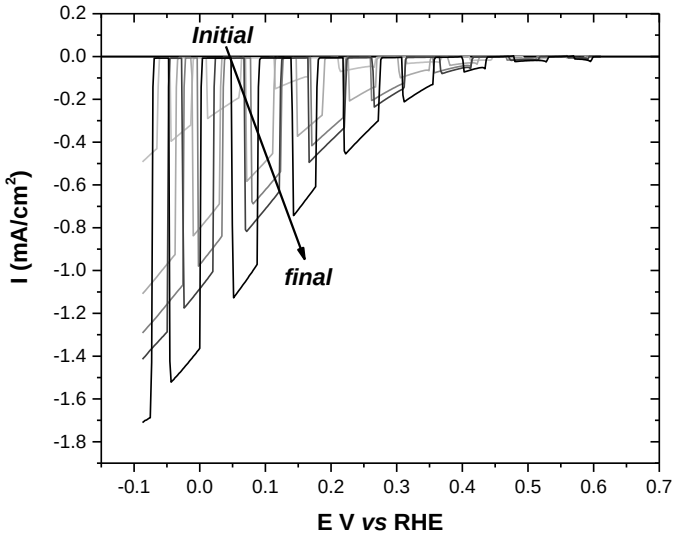

Figure S11. Activation process of NiO/PCDTBT:PCBM/TiO_2/RuO_2-NP by performing J-V curves at pH 7, back illumination. (Area = 0.7 cm^2).

Table S1: Literature review on organic photocathodes.

Entry	HTL	Active Layer	ETL	Catalyst	Stability	Current Onset (vs RHE)	Current (mA/cm^2) 0 RHE	pH	Ref
1	NiO	PCDTBT:PCBM	ALD-TiO_2	RuO_2-NP	-10 % in 5 hours (@ 0 vs RHE)	0.67	1.4	7	In this work
2	PEDOT	PCDTBT:PCBM	ALD-TiO_2	RuO_2-NP	95 % in 90 min (@ 0 V vs RHE)	0.67	2.9	7	In this work
3	CuI	P3HT:$PC_{60}BM$	TiO2-ALD	RuOx	3.5 hours (@ 0 V vs RHE)	0.5	3	5	6
4	CuI	P3HT:$PC_{60}BM$	TiO2-PEI	Pt	-40% in 40 min (@ 0 vs RHE)	0.60	5.25	1.0	7
5	p-MoS_2	P3HT:$PC_{60}BM$	TiO_2	MoS_3	-50% in 5 min (@ 0 vs RHE)	0.56	1.21	1.0	8
6	WO_3	P3HT:$PC_{60}BM$	TiO_2	Pt	-30% peak in 8h (@ 0.20 vs RHE)	0.56	2.48	1.4	9
7	PEDOT:PSS	P3HT:$PC_{60}BM$		MoS_3	-100% <15 min (@ 0 vs RHE) [a]	-0.15	0.05	2	10
8		P3HT:$PC_{60}BM$		MoS_3	NA	0.19	0.6	2	10
9	rGO	P3HT:$PC_{60}BM$		MoS_3	No loss in 1h	0.20	0.7	2	10
10	NiO_x (sol. gel.)	P3HT:$PC_{60}BM$		MoS_3	+100% in 1h (@ 0 vs RHE)[b]	0.34	1.3	2	10
11	MoO_x (sol. gel.)	P3HT:$PC_{60}BM$		MoS_3	-20% in 1h (@ 0 vs RHE)	0.41	2.2	2	10
12	PEDOT:PSS	α-6T/SubPc	C_{60}	MoS_3	-90% in 5min (@ 0 vs RHE)			0-1	11
13	PEDOT:PSS	α-6T/SubNc	C_{60}	MoS_3	-30% in 5min (@ 0 vs RHE)	0.69	3.6	0-1	11
14	PEDOT:PSS	α-6T/ SubNc/SubPc	C_{60}	MoS_3	-70% in 5min (@ 0 vs RHE)	0.70	1.5	0-1	11
15	PEDOT:PSS	α-6T/α-6T: SubNc/SubNc	C_{60}	MoS_3	-90% in 5min (@ 0 vs RHE)	0.68	2.4	0-1	11
16	MoO_3	P3HT:$PC_{60}BM$	TiO_2	Pt	-80% in 30min (@ 0.18 vs RHE)	~0.6	~1.5	1.37	12
17		P3HT:$PC_{60}BM$	TiO_2	Pt	No loss in100min[c,d]			1.37	13
18	MoO_3	P3HT:$PC_{60}BM$	TiO_2	Pt	-90% in 100min (@ 0 vs RHE)[c,e]	~0.55	~3	1.37	13
19	CuI	P3HT:$PC_{60}BM$	TiO_2	Pt	-60% in 20min	0.72	~8	1	14

					(@ 0 vs RHE)				
20	PANI	P3HT:$PC_{60}BM$			-70% in 1h (@ 0 vs RHE)	0.1	0.3	2	15
21	PEDOT:PSS	P3HT:$PC_{60}BM$	AZO	C-Pt	-60% in 1h	~0.25	~1.2	7	16
22	PEDOT:PSS	P3HT:$PC_{60}BM$	LiF/Al (evap)	Ti- MoS_3	-45% in 10 min (@ 0 vs RHE) [a]	0.48	8.47	0-1	17
23	PEDOT:PSS	P3HT:$PC_{60}BM$	LiF/Al (evap)	Ti-Pt/C	NA	0.67	7.87	0-1	17
24	PEDOT:PSS	P3HT:$PC_{60}BM$		Ti- MoS_3	-12% in 10 min (@ 0 vs RHE) [a]	0.32	6.81	0-1	17
25	PEDOT:PSS	P3HT:$PC_{60}BM$	C_{60}	C_{60}-MoS_3	-60% in ~1 min (@ 0 vs RHE) [a]	0.24	0.86	0-1	17
26	Crosslinked-PEDOT	P3HT:$PC_{60}BM$	TiO_x (sol.gel)	Platinum	No loss >3h	>0.2	<0.4	2	18
27		P3HT		Pt	NA	~0.24	~0.04	~1	19
28	PEDOT:PSS	P3HT	C_{60}	Co-N_3	Stable 1h	>0.3	~0.002	4.5	20
29	Au	CdSe:P3HT		Pt	-50% in 5h	~0.8	1.2	7	21
30		ZnPc/C_{60} (bilayer)		Pt		~0	Negligible	2	22
31		P3HT			No observed photocurrent degradation-hours		~0.015	1	23
32	PEDOT:PSS	P3HT:$PC_{60}BM$	MoS_3 (np. suspension)	MoS_3	-50% in 45 min (@ 0.16 vs RHE)[a]	0.25	0.05	~0	24
33	PEDOT:PSS	P3HT:$PC_{60}BM$	TiO2 (np. suspension)		NA	0.45	~0.1	~0	24
34	PEDOT:PSS	P3HT:$PC_{60}BM$	TiO2/ MoS_3 (np. suspension)	MoS_3	-30% in 45 min (@ 0.16 vs RHE)[a]	0.45	~0.2	~0	24
35		H_2Pc:C_{60} (bilayer)		Pt	NA	~0.3	~0.05	2	25
36		P3HT: Dy@C_{82}			Stable over 1h (@ OCP)	~0.7	~0.012	6.5	26
37		P3HT: Dy@C_{82}			Stable over 1h (@ OCP)	~0.6	~0.008[e]	~6.5	27
38		P3HT			-10% over 2h	~0.1	Negligible[e]	4.0	28
39		Poly(pyrrole)				~0.2	~0.002	~2	29

[a]Only surface of photocathode in contact with water. [b]Performance increases in first few minutes and then plateaus [c]Performance first increases and then decreases [d]-50% in 90min from peak. [e]monochromatic light.

F. References:

1. K.-H. Chang and C.-C. Hu, *Electrochem. Solid-State Lett,* 2004. **7,** A466-A469.

2. S. Wheeler, F. Deledalle, N. Tokmoldin, T. Kirchartz, J. Nelson and J. R. Durrant, *Phys. Rev. Appl.*, 2015, **4**, 024020.

3. S. R. Cowan, J. V. Li, D. C. Olson and E. L. Ratcliff, *Adv. Energy Mater.*, 2015, **5**, 1400549.

4 H. Cheng Wong, Z. Li, C. Hong Tan, H. Zhong, Z. Huang, H. Bronstein, I. McCulloch, ao T. Cabral and J. R. Durrant, *ACS Nano*, 2014, **8**, 1297-1308.

5 L. Steier, J. Luo, M. Schreier, M. T. Mayer, T. Sajavaara and M. Grätzel, *ACS Nano*, 2015, **9**, 11775–11783.

6 L. Steier, S. Bellani, H. C. Rojas, L. Pan, M. Laitinen, T. Sajavaara, F. Di Fonzo, M. Grätzel, M. R. Antognazza and M. T. Mayer, *Sustain. Energy Fuels*, 2017, 1915–1920.

7 H. C. Rojas, S. Bellani, E. A. Sarduy, F. Fumagalli, M. T. Mayer, M. Schreier, M. Grätzel, F. Di Fonzo and M. R. Antognazza, *ACS Omega*, 2017, **2**, 3424–3431.

8 S. Bellani, L. Najafi, A. Capasso, A. E. Del Rio Castillo, M. R. Antognazza and F. Bonaccorso, *J. Mater. Chem. A*, 2017, **5**, 4384–4396.

9 A. Mezzetti, F. Fumagalli, A. Alfano, D. Iadicicco, M. R. Antognazza and F. di Fonzo, *Faraday Discuss.*, 2017, **198**, 433–448.

10 T. Bourgeteau, D. Tondelier, B. Geffroy, R. Brisse, S. Campidelli, R. Cornut and B. Jousselme, *J. Mater. Chem. A*, 2016, **4**, 4831–4839.

11 A. Morozan, T. Bourgeteau, D. Tondelier, B. Geffroy, B. Jousselme and V. Artero, *Nanotechnology*, 2016, **27**.

12 A. Ghadirzadeh, F. Fumagalli, A. Mezzetti, S. Bellani, L. Meda, M. R. Antognazza and F. Di Fonzo, *ChemPhotoChem*, 2018, **2,** 1-11.

13 F. Fumagalli, S. Bellani, M. Schreier, S. Leonardi, H. C. Rojas, A. Ghadirzadeh, G. Tullii, A. Savoini, G. Marra, L. Meda, M. Grätzel, G. Lanzani, M. T. Mayer, M. R. Antognazza and F. Di Fonzo, *J. Mater. Chem. A*, 2016, **4**, 2178–2187.

14 H. C. Rojas, S. Bellani, F. Fumagalli, G. Tullii, S. Leonardi, M. T. Mayer, M. Schreier, M. Grä, G. Lanzani, F. Di Fonzo and M. R. Antognazza, *Energ. Environ. Sci.* 2016, **9**, 3710.

15 E. Belarbi, V. M. Blas-Ferrando, M. Haro, H. Maghraoui-Meherzi and S. Gimenez, *Chem. Eng. Sci.*, 2016, **154**, 143-149.

16 M. Haro, C. Solis, V. M. Blas-Ferrando, O. Margeat, S. Ben Dhkil, C. Videlot-Ackermann, J. Ackermann, F. Di Fonzo, A. Guerrero and S. Gimenez, *ChemSusChem*, 2016, **9**, 3062–3066.

17 T. Bourgeteau, D. Tondelier, B. Geffroy, R. Brisse, R. Cornut, V. Artero and B. Jousselme, *ACS Appl. Mater. Interfaces*, 2015, **7**, 16395-16403.

18 M. Haro, C. Solis, G. Molina, L. Otero, J. Bisquert, S. Gimenez and A. Guerrero, *J. Phys. Chem. C*, 2015, **119**, 6488-6494.

19 G. M. Suppes, P. J. Fortin and S. Holdcroft, *J. Electrochem. Soc.*, 2015, **162**, H551–H556.

20 Y. Chen, H. Chen and H. Tian, *Chem. Commun.*, 2015, **51**, 11508–11511.

21 L.-H. Lai, W. Gomulya, M. Berghuis, L. Protesescu, R. J. Detz, J. N. H. Reek, M. V. Kovalenko and M. a.

Loi, *ACS Appl. Mater. Interfaces*, 2015, **7**, 19083–19090.

22 T. Abe, Y. Hiyama, K. Fukui, K. Sahashi and K. Nagai, *Int. J. Hydrogen Energy*, 2015, **40**, 9165–9170.

23 G. Suppes, E. Ballard and S. Holdcroft, 2013, **4**, 5345-5350.

24 T. Bourgeteau, D. Tondelier, B. Geffroy, R. Brisse, C. Laberty-Robert, S. Campidelli, R. de Bettignies, V. Artero, S. Palacin and B. Jousselme, *Energy. Sustain. Soc.*, 2013, **6**, 2706–2713.

25 T. Abe, S. Tobinai, N. Taira, J. Chiba, T. Itoh and K. Nagai, *J. Phys. Chem. C*, 2011, **115**, 7701–7705.

26 S. Yang, L. Fan and S. Yang, *J. Phys. Chem. B,* 2004, **108**, 4394-4404.

27 S. Yang, L. Fan and S. Yang, *Chem. Phys. Lett.*, 2004, **388**, 253-258.

28 O. A. El-Rashiedy and S. Holdcroft, *J. Phys. Chem.* 1996, **100**, 5481-5484.

29 M. Kaneko, K. Okuzumi and A. Yamada, *J. Electroanal. Chem. Interfacial Electrochem.*, 1985, **183**, 407–410.